Curved Grating Fabrication Techniques for Concentric-Circle Grating, Surface-Emitting Semiconductor Lasers

Rebecca H. Jordan, Oliver King, Gary W. Wicks, Dennis G. Hall
The Institute of Optics, University of Rochester, Rochester NY 14627

Erik H. Anderson
*IBM T. J. Watson Research Center, Yorktown Heights, NY 10598, and
Lawrence Berkeley Laboratory, Berkeley, CA 94720*

Michael J. Rooks
National Nanofabrication Facility, Cornell University, Ithaca NY 14853

Abstract

We describe the fabrication and operational characteristics of a novel, surface-emitting semiconductor laser that makes use of a concentric-circle grating to both define its resonant cavity and to provide surface emission. A properly fabricated circular grating causes the laser to operate in radially inward- and outward-going circular waves in the waveguide, thus introducing the circular symmetry needed for the laser to emit a beam with a circular cross-section. The basic circular-grating-resonator concept can be implemented in any materials system; an AlGaAs/GaAs graded-index, separate confinement heterostructure (GRINSCH), single-quantum-well (SQW) semiconductor laser, grown by molecular beam epitaxy (MBE), was used for the experiments discussed here. Each concentric-circle grating was fabricated on the surface of the AlGaAs/GaAs semiconductor laser. The circular pattern was first defined by electron-beam (e-beam) lithography in a layer of polymethylmethacrylate (PMMA) and subsequently etched into the semiconductor surface using chemically-assisted (chlorine) ion-beam etching (CAIBE).We consider issues that affect the fabrication and quality of the gratings. These issues include grating design requirements, data representation of the grating pattern, and e-beam scan method. We provide examples of how these techniques can be implemented and their impact on the resulting laser performance. A comparison is made of the results obtained using two fundamentally different electron-beam writing systems. Circular gratings with period $\Lambda = 0.25$ μm and overall diameters ranging from 80 μm to 500 μm were fabricated. We also report our successful demonstration of an optically pumped, concentric-circle grating, semiconductor laser that emits a beam with a far-field divergence angle that is less than one degree. The emission spectrum is quite narrow (less than 0.1 nm) and is centered at wavelength $\lambda = 0.8175$ μm.

I. Introduction

Curved grating structures have a considerable number of potentially interesting uses in the field of integrated optics, such as in-plane focusing elements, focusing input/output couplers, and various laser resonator designs employing curved gratings for feedback and surface emission. Although some of these applications have been proposed in the past, they have not gained general acceptance in large part because of the difficulty in fabricating such structures (1, 2). However, a surge of interest in the use of concentric circles as the grating elements in distributed feedback or distributed Bragg reflector laser structures (DFB and DBR) has occurred recently (3, 4, 5, 6, 7). A properly fabricated circular grating causes the laser to operate in radially inward- and outward-going circular waves in the waveguide, thus introducing the circular symmetry needed for the laser to emit with a circular cross-section. In this paper we report our successful demonstration of an optically pumped, concentric-circle grating, semiconductor laser (CCGSE) that emits a beam with a far-field divergence angle that is less than one
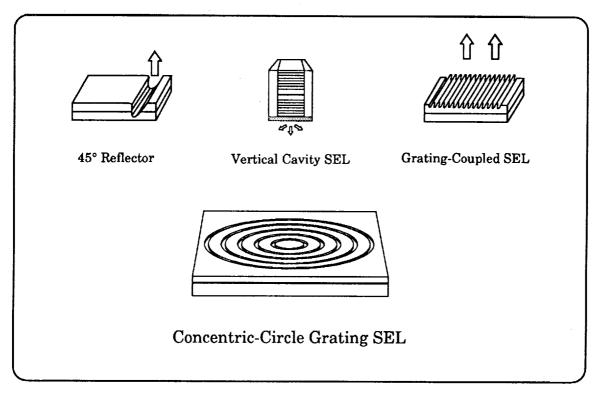

Figure 1. Types of surface-emitting lasers: (a) 45 degree reflector, (b) vertical-cavity surface-emitting laser, (c) grating-coupled surface-emitting laser, and (d) concentric-circle grating, surface-emitting semiconductor laser.

degree. The emission spectrum is quite narrow (less than 0.1 nm) and is centered at wavelength $\lambda = 0.8175$ μm. In addition to these features, other fabrication and performance advantages inherent in surface-emitting geometries, such as wafer-scale testing, are available for the CCGSE laser. The CCGSE lasers are particularly well suited for array operation. A large, phase-locked array of the devices could produce an exceptionally narrow, high power, single mode beam. Figure 1 shows schematics of several surface-emitting laser geometries: the 45 degree reflector, the vertical cavity surface-emitting laser, the grating coupled surface-emitting laser, and the CCGSE laser.

This paper focuses on the techniques employed to fabricate the grating element of our recently demonstrated concentric-circle grating surface-emitting semiconductor laser (8). We give particular attention to the use of electron-beam (e-beam) lithography for the definition of the grating rings, and consider how best to approach the problem of defining and writing features with circular symmetry in the Cartesian environment of an e-beam pattern generator.

II. Concentric–Circle Surface–Emitting Lasers

A schematic representation of the CCGSE laser is shown in Figure 2. The semiconductor material consisted of a graded-index, separate-confinement heterostructure (GRINSCH) quantum well laser structure. The undoped, molecular-beam-epitaxy (MBE) grown epi-layers consisted of a 1.5μm thick $Al_{0.85}Ga_{0.15}As$ lower cladding layer, a 0.3μm thick parabolically graded region with a 100Å thick quantum well, and a 0.25μm thick $Al_{0.85}Ga_{0.15}As$ upper cladding layer. The thin, high-aluminum-concentration upper clad allows for efficient continuous-wave (cw) optical pumping with the 5145Å line of an Argon-ion laser as well as a strong coupling between the grating and the TE_0 guided mode. In this structure a circular grating comprised of concentric rings is used to define the resonator cavity. The grating serves both to provide feedback to the cavity waveguide modes, which propagate inwardly and outwardly along the radial direction, and to couple these guided modes to radiation modes propagating normal to the surface of the waveguide. The resulting emission from a properly operating laser has the form of a narrowly diverging beam with circular cross-section and narrow wavelength spectrum.

All the gratings shown in this paper were written by either the JEOL JBX-5DII e-beam system at the National Nanofabrication Facility at Cornell University, or an IBM Vector Scan 6 (VS-6) system equipped with a real-time polar-to-rectangular coordinate conversion system (9). In each case the patterns were written in a 1500Å thick layer of polymethylmethacrylate (PMMA) resist. The
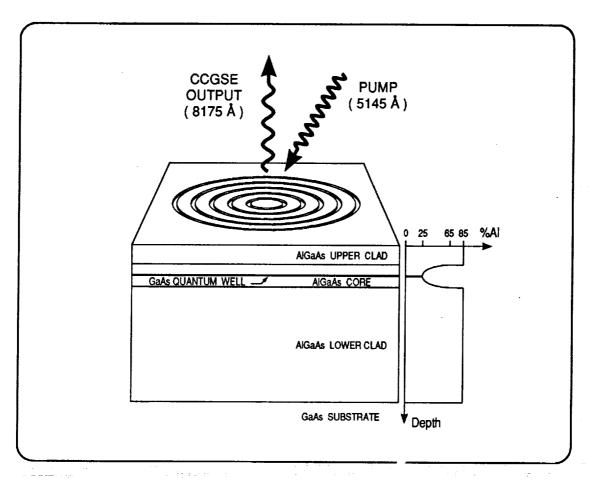
Figure 2. Schematic drawing of the concentric-circle grating, surface-emitting semiconductor laser, showing the AlGaAs/GaAs epitaxial layer structure. The circular grating etched into the AlGaAs/GaAs laser structure provides cavity feedback and coupling for surface emission. Pump power is provided by a cw Argon-ion laser operating at 5145Å.

resulting developed pattern was etched into the underlying semiconductor laser material using chemically assisted ion-beam etching (CAIBE) with chlorine as the reactive species (10). The etched depth of the gratings varied from 800 Å to as deep as 3500 Å. A 3500 Å deep grating is shown in Figure 3.

In order to characterize the performance of the completed lasers the substrate was lapped to a thickness of 100μm, soldered to a gold-plated alumina substrate, and mounted in a dewar held at 77° K. The lasers were then excited by a continuous-wave Argon-ion laser pump beam. The laser's near- and far-field patterns were monitored with a silicon CCD camera and the spectrum was collected by a 0.75 meter spectrometer and photomultiplier tube.

The requirements for such a grating present a considerable fabrication challenge. To provide optimum feedback, the period Λ of the grating must be 0.25 μm, and the grating must posssess a 1:3 peak-to-trough ratio (25% duty-cycle, where a grating trough representing the "on" state). While the precise value of the peak-to-trough ratio is not crucial, the relative variation of this ratio within a completed grating is crucial. Even slight variations in the ratio with respect to the grating's azimuthal angle will destroy the circular nature of the lasing modes (11). Not only must the linewidth variation be held to under one percent, the grating lines must maintain this required phase relationship over a circular field having a diameter of at least 100 μm.
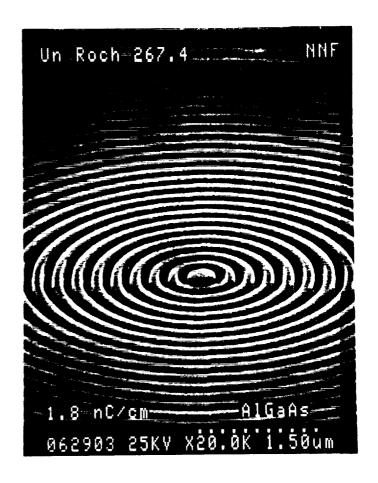

Figure 3. Scanning electron micrographs of a 0.25μm period concentric-circle grating. The grating has been etched to a depth of 3500Å using chemically assisted ion-beam etching.

Although it might seem initially that holographic exposure techniques are a reasonable alternative to e-beam lithography, in practice this is a difficult approach. To produce a holographic pattern consisting of equally spaced rings with roughly constant amplitude and fringe visibility, a plane wave and a conical wave must be interfered (mixed). Two methods for forming conical waves present themselves(12, 13), but the cone angle necessary to achieve the period required for this application is so severe as to preclude the use of conventional optics. It should be pointed out that while methods for producing straight line gratings ordinarily rely on a large spatial separation of the interfering beams to achieve large interference angles and, hence,

appropriately small periodicities, this separation is not easily achieved in two dimensions.

III. Grating Data Representation

A primary consideration in the problem of writing curved line structures by e-beam lithography is the question of how best to describe curved features with an XY (Cartesian) digital-to-analog converter (DAC) pattern generator. We consider three
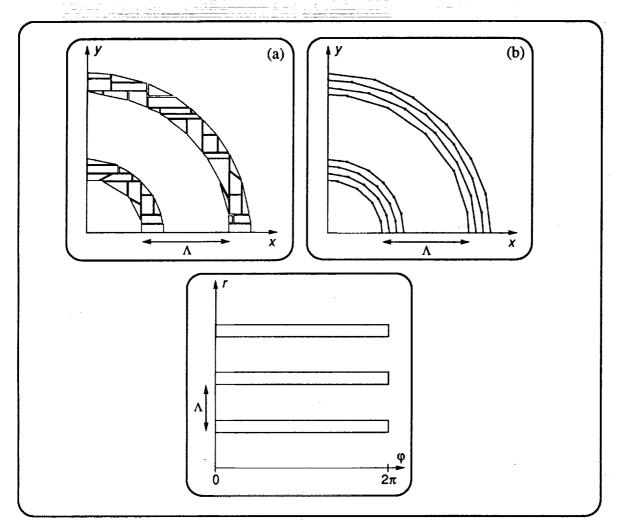

Figure 4. Examples of the three approaches for data representation of the curved gratings. (a) An example of the JEOL fractured-polygon representation of an arc segment. (b) A portion of a circular grating as represented by single-pass-line segments in the JEOL system. The endpoints of each line segment are staggered with respect to those of its neighbors in order to more closely approximate a circle. (c) The radius versus angle (r vs θ) polar data representation used by the IBM Vector Scan 6 e-beam machine.

possibilities here, two of which have been implemented on the JEOL machine and the other on the IBM VS-6.

The least workable of these solutions makes use of a fractured polygon representation of curved line segments, as implemented on the JEOL machine. Here, a best fit of rectangles and triangles is made to the ideal arc segment. An example is shown in Figure 4(a). This technique, however, leads to two unacceptable difficulties. The first arises from the problem of accurately exposing small features with dimensions approaching the 25 Å grid of pixels to which the beam is addressed. The resulting developed rings tend to have scalloped edges and, hence, local variations in linewidth. Of equal concern is the very large amount of data generated using this scheme. The disk space required grows with the square of the number of rings generated, and easily becomes unwieldy.

A second method used with the JEOL machine utilizes rings comprised of many single-pass-line segments as demonstrated in Figure 4(b). For these gratings, four single-pass-line rings were used to approximate a single grating period. The length of each line segment was determined by setting a maximum allowed radial deviation of the segment, or chord, from the ideal circle. In order to more closely approximate a circle rather than a many-sided polygon, the starting position of each single-pass-line segment was shifted in relation to its neighboring line-segment circles. Additionally, in an effort to eliminate any angular correlations, the starting
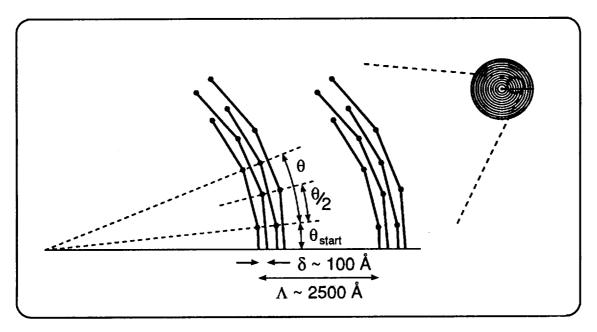

Figure 5. An enhanced detail of the JEOL single-pass line technique, showing the staggered onset of the single pass lines with respect angular location.

229

position of each group of four rings that define a grating period is shifted in angle by some small, random amount. This is shown in greater detail in Figure 5. When using the single-pass-line technique, particular care must be taken to specify the correct dose. Although the ring data is specified in terms of line segments, exposures are actually performed by mapping the line, in a pixel-wise fashion, onto a Cartesian grid. As a result, the exposed points along a 45° line, for example, are therefore more widely spaced than those of a line at 0°. In order to correctly expose lines which deviate from the Cartesian coordinate axes by an angle θ, a 1/cos(θ) dose correction must be applied in order to compensate for the corresponding geometrical increase in the inter-pixel spacing along the line. JEOL has provided us with a customized exposure program which allows the user to assign dose corrections as a function of angle.

Of the pattern generation techniques attempted on the JEOL, the use of angular dose corrections has shown the most promise for generating circular lasing modes, as shown in Figure 6(a). However, to date the JEOL still has not produced devices with true circular lasing modes. Without the customized JEOL software, the patterning system will separate the pattern into 9° wedges. Each wedge will have a slightly different duty cycle, or peak-to-trough ratio, and the laser will operate with one independent linear mode corresponding to each wedge. As an example, Figure 6(b) shows lasing along the four radial directions with the smallest

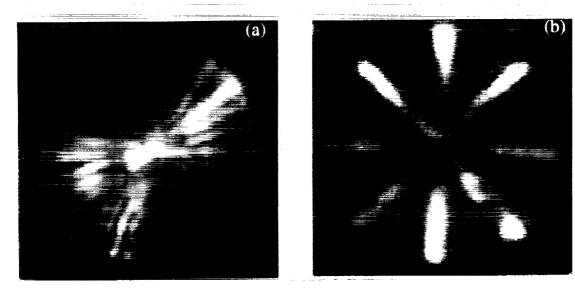**Figure 6**. (a) An image of the near-field of a 160μm diameter laser defined by the JEOL system using a single field with a 1/cos(θ) dose correction applied. (b) A 240μm diameter laser with the default angular dose correction applied. The laser operates in several independent linear modes.
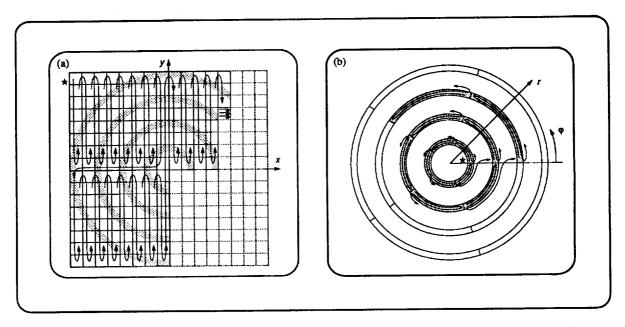
Figure 7. A drawing of the two types of scan format. (a) The rectangular, raster-scan format used by the JEOL e-beam machine, and (b) the polar scan format used by the IBM Vector-Scan 6 e-beam machine.

line-to-space ratios. Unfortunately, the additional information required to ensure the correct exposure and eliminate as much angular correlation in the pattern as possible results in file sizes which approach those generated by the fractured polygon technique.

A more practical approach to this problem has been implemented on an IBM VS-6 machine equipped with a real-time polar-to-rectangular coordinate conversion system. This system makes good use of the inherent angular symmetry in circular structures. Here, the pattern file specifies radius as a function of angle. A representation of this is shown in Figure 4(c). This information is then converted to Cartesian coordinates in real time utilizing hardware sine- and cosine-lookup tables. For this method, no exposure correction is needed to maintain a fixed linewidth since the line dose determined for the polar representation is preserved during the coordinate transformation. The use of the VS-6 system allows for a significant reduction in the size of the stored data set in comparison to the JEOL representations. For example, a 300 period, 150μm diameter grating requires 14 megabytes of disk storage if using the JEOL system, whereas the VS-6 system format occupies only 278 kilobytes. Additionally, there is a corresponding decrease in the length and complexity of the pre-exposure computing tasks.

IV. Scan Format

Another issue critical to the successful fabrication of CCGSE lasers is the choice of scan format. In the case of the JEOL machine, the grating pattern is segmented into rectangular fields and sub-fields for exposure. The grating is then written sub-field by sub-field within a given field. At the completion of each field the sample stage is moved to the next field, and so on. An example of this raster-scan technique is shown in Figure 7(a). A worst case example of the results of this technique is shown in Figure 8. Figure 8 shows the near-field of a 160 μm diameter laser consisting of 80 μm × 80 μm fields filled by 10 μm × 10 μm sub-fields. Clearly, there are significant errors in the phase and/or linewidth of the grating at the boundaries between
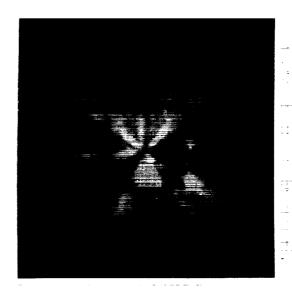

Figure 8. An image of the near-field of a 240 μm diameter laser having significant field (80 μm × 80 μm) and sub-field (10 μm × 10 μm) stitching errors. This grating was written by the JEOL machine using the single-pass line technique.

both fields and sub-fields, as evidenced by the local variations in the intensity of the emitted radiation. The hardware involved in scanning this pattern includes an interferometrically controlled stage, a set of DACs used for deflection to a sub-field within a field, and a second set of DACs used for deflection within the sub-field. We attribute the grating errors to an imperfect match between these components due to inaccuracies in calibration as well as any drift incurred during the time interval required to expose a given field/ sub-field.

In comparison, the VS-6 machine scans the grating in a polar, rather than rectangular, fashion, as shown in Figure 7(b). Again, two sets of DACs are used, the first of which addresses the beam to the neighborhood of the next shape to be filled (in this case, an arc-segment), while the second performs the fill. The order of exposure is different, however, as abutting arc-segments making up a ring are written sequentially and each ring is completed before moving to the next period. As a result, there is a diminished likelihood of introducing abrupt local errors in the phase or linewidth. The near- and far-field radiation patterns of a laser made using this method are shown in Figure 9. This 150μm diameter grating was written in a single field, one ring at a time, beginning with the center ring of the grating. The

near-field emission is circular with no apparent local non-uniformities, indicating lasing in the desired, lowest order circular modes. In the far-field, a narrowly diverging (< 1 degree), circular beam results. This laser's radiation spectrum, centered on 8175 Å, had width less than 0.1 nm.

V. Conclusions

The problem of writing sub-micron period curved gratings is sufficiently difficult that producing patterns of the quality necessary for applications such as CCGSE lasers requires hardware and software designed with such applications in mind. When writing large, complex structures, it may not be practical to store the data required to completely specify the pattern in a Cartesian representation. Other techniques, such as using real-time hardware coordinate conversions or dedicated fast processors to calculate coordinates in real time, are viable alternatives. Additionally, care must be taken to design exposure hardware that can scan reasonably large fields with sufficiently low distortion, and with sufficient resolution and stability. If these criteria are met, as they are in the IBM VS-6, it is possible to fabricate a CCGSE laser which oscillates in circular modes and produces a good quality, narrowly diverging, circular beam with a relatively narrow wavelength spectrum. This CCGSE semiconductor laser is a ver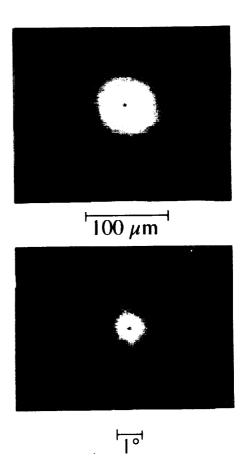y tough test for the fabrication technology, since the grating itself determines the lowest threshold mode in which the laser will oscillate. A grating that does not meeting the exacting fabrication requirements does not just reduce lasing efficiency, it changes fundamentally the way the laser operates.

Figure 9. (a) Top. An image of the near-field of a 150 μm diameter laser written by the IBM VS-6 machine. Note the uniform, circular nature of the emission. (b) Bottom. The resulting beam profile in the far-field. The beam divergence angle is less than 1°.

References

1. P. K. Tien, *Optics Letters* **1**, 64 (1977).

2. G. I. Hatakosi, H. Fujoma, K. Goto, *Applied Optics* **23**, 1749 (1984).

3. T. Erdogan, D. Hall, *Journal of Applied Physics* **68**, 1435-1444 (1990).

4. T. Erdogan, D. G. Hall, *IEEE Journal of Quantum Electronics* **28**, (1991).

5. R. M. Schimpe, US Patent No. 4,743,083, (1988).

6. C. Wu, T. Makino, J. Glinski, R. Maciejko, S. I. Najafi, *Journal of Lightwave Technology* **9**, 1264-1277 (1991).

7. X. H. Zheng, *Electronics Letters* **25**, 1311-12 (1989).

8. T. Erdogan, et al., *Applied Physics Letters* , (1992).

9. D. Kern, et al., *Proceedings of the SPIE* **447**, 204 (1984).

10. R. C. Tiberio, et al., *Journal of Vacuum Science and Technology B* **9**, 2842 (1991).

11. T. Erdogan, et al., *Applied Physics Letters* **60**, 1773-1775 (1992).

12. Q. S. Ru, N. Ohyama, T. Honda, J. Tsujiuchi, *Optics Communications* **67**, 195-188 (1988).

13. M. V. Perez, C. Gomez-Reino, J. M. Cuadrado, *Optica Acta* **33**, 1161-1176 (1986).